A comparison of different methods for fitting susceptibility data of cobalt(II) coordination polymers in a new cobalt(II)/sulfate 1-D chain

Leigh F. Jones, Colin A. Kilner and Malcolm A. Halcrow*

Received (in Durham, UK) 22nd January 2007, Accepted 2nd May 2007
First published as an Advance Article on the web 6th June 2007
DOI: 10.1039/b700987a

The 1-D chain polymer $[\{Co(\mu\text{-}SO_4)\mathbf{L}_3\}_n]$ (**L** = 3{5}-*tert*-butylpyrazole) was prepared by the reaction of $CoSO_4 \cdot 7H_2O$ with 3 equiv. of **L** in MeOH. The complex contains trigonal bipyramidal cobalt(II) centres with two axial *O*,*O*′-bridging sulfato ligands. The resultant linear chains are arranged into an approximately hexagonal array, the molecules being well-separated from each other by a honeycomb of interdigitated *tert*-butyl groups. Susceptibility data from $[\{Co(\mu\text{-}SO_4)\mathbf{L}_3\}_n]$ are consistent with an antiferromagnetic Curie–Weiss chain, which could be well-interpreted using Heisenberg 1-D treatments. Three approaches to model these data were studied to try and separate superexchange and zero-field splitting effects. A recently proposed empirical approach gave *g* and *J* values in excellent agreement with a $S = \frac{3}{2}$ Heisenberg chain model, as long as the latter was performed using only high temperature data, which are not affected by zero-field splitting.

Introduction

Interpretation of magnetic susceptibility data from polynuclear, high-spin cobalt(II) species is complicated by the co-existence of weak superexchange ($|J| < 20$ cm^{-1})[1] and strong zero-field splitting (ZFS, $|D| > 20$ cm^{-1}),[2] which are often of similar magnitude.[3] It then becomes difficult to model *J* and *D* independently from an isotropic susceptibility curve, particularly in an antiferromagnetic system, since one effect cannot be treated as a small perturbation of the other. Mathematical treatments of this problem applicable to specific polynuclear cluster structures are available.[4,5] However, for 1-D cobalt(II) coordination polymers, three different approaches to deriving magnetic parameters from powder susceptibility data have been commonly used. First are models treating the compound as an isotropic Heisenberg chain of classical $S = \frac{3}{2}$ spins. Equations derived by Fisher[6] and Hatfield *et al.*[7] to describe this situation are commonly employed,[8] but the resultant *J* values may be contaminated by ZFS effects, which are not treated in this approach. Moreover, chain complexes of octahedral cobalt(II) centres, the most common coordination geometry for this metal ion, have a triplet ground state with significant orbital angular momentum, which is poorly described by an isotropic model.[9,10] Numerical models of superexchange in cobalt(II) chains with Ising or XY magnetic anisotropy are impractical for routine magnetochemical analyses.[1] A second approach is to argue that if *D* is large and negative, only the lowest lying $m_S = \pm\frac{1}{2}$ sub-levels will be populated at sufficiently low temperatures (typically assumed to be below 30 K).[4,9] Analytical expressions for magnetically isotropic or anisotropic 1-D chains with $S = \frac{1}{2}$ spins[1] have been used to derive *J* independently of *D*, for the putative $m_S = \frac{1}{2}$ chains described by the low temperature data.[11] Finally, a more recent qualitative treatment proposed by Rueff *et al.* describes the deviation of the material from Curie behaviour using two different exponential terms, one of which contains contributions from *J* and the other from *D*.[12] Despite its empirical origins, the simplicity of the Rueff approach has led to it finding increasing use.[12,13]

As a continuation of our investigations of polynuclear and supramolecular complexes formed by 3{5}-substituted pyrazole ligands,[14–17] we have prepared $[\{Co(\mu\text{-}SO_4)\mathbf{L}_3\}_n]$ (**L** = 3{5}-*tert*-butylpyrazole, **1**). This compound crystallises as well separated coparallel cobalt sulfate chains, making it an ideal test bed for 1-D magnetic behaviour. We have compared the utility of all three of the above treatments in the analysis of the susceptibility data, making this the first test of Rueff's qualitative approach to this problem against other methods.

Results and discussion

Treatment of $CoSO_4 \cdot 7H_2O$ with 3 equiv. of **L**[18] in MeOH at room temperature yielded a purple solution, which was filtered and concentrated *in vacuo*. Slow diffusion of diethyl ether vapour into this mixture yielded analytically-pure purple crystals of **1** in 45% yield. The crystal structure of **1** shows cobalt(II) centres exhibiting a trigonal bipyramidal stereochemistry, with three pyrazole N-donors in the equatorial plane (Table 1, Fig. 1). This geometry is slightly distorted [$\tau = 0.791(4)$[19]] by the wide equatorial N(2)–Co(1)–N(11) angle, which is presumably imposed by the geometric requirements of the hydrogen bonds donated by these two pyrazole groups (see below). The axial sites in the coordination sphere are occupied by O-donors from two different *O*,*O*′-bridging sulfate ligands, which link the metal ions into 1-D chains running parallel to the crystallographic b-axis. Adjacent cobalt ions in the chains are related by crystallographic 2_1 operations (Fig. 2) and are separated by 6.5894(1) Å.

School of Chemistry, University of Leeds, Woodhouse Lane, Leeds, UK LS2 9JT. E-mail: m.a.halcrow@leeds.ac.uk

Table 1 Selected bond lengths (Å) and angles (°) in the crystal structure of **1**

Co(1)–N(2)	2.0342(16)	Co(1)–O(30)	2.1228(13)
Co(1)–N(11)	2.0315(16)	Co(1)–O(33^{i})	2.0835(14)
Co(1)–N(20)	2.0483(15)		
N(2)–Co(1)–N(11)	126.49(6)	N(11)–Co(1)–O(30)	88.01(6)
N(2)–Co(1)–N(20)	116.99(7)	N(11)–Co(1)–O(33^{i})	87.46(6)
N(2)–Co(1)–O(30)	92.38(6)	N(20)–Co(1)–O(30)	86.75(6)
N(2)–Co(1)–O(33^{i})	87.08(6)	N(20)–Co(1)–O(33^{i})	98.88(6)
N(11)–Co(1)–N(20)	116.45(7)	O(30)–Co(1)–O(33^{i})	173.94(5)

Symmetry code: (i) $1-x, -\frac{1}{2}+y, \frac{3}{2}-z$.

Each **L** ligand in **1** donates an intramolecular hydrogen bond to an O atom from a sulfate ligand bound to the same cobalt ion. Two of these are donated to the two non-coordinated O atoms from the same sulfate ligand while the third involves one of these O atoms on the other symmetry-related ligand (Fig. 1 and Fig. 2). Hence, one O atom on each sulfate ligand accepts two hydrogen bonds from different $[Co\mathbf{L}_3]^{2+}$ centres while the other accepts one, and the pyrazole NH groups on each cobalt centre in a chain are disposed in the same head-to-head-to-tail orientation. Neighbouring chains in the crystal pack by interdigitating their *tert*-butyl groups, forming a near-hexagonal array of coparallel cobalt sulfate chains embedded in a hydrophobic honeycomb (Fig. 3). The closest distances between neighbouring cobalt sulfate chains in the lattice range from Co(1)···O(31^{ii}) = 8.2973(14) to Co(1)···O(31^{iii}) = 10.2164(15) Å (symmetry codes: (ii) $\frac{1}{2}+x, \frac{1}{2}-y, 1-z$; (iii) $\frac{1}{2}-x, 1-y, \frac{1}{2}+z$). The fact that the paramagnetic chains in this material are so well isolated means that magnetic dipolar or superexchange interactions between chains should be minimal.

A powder sample of **1** exhibits $\chi_M T = 2.3$ cm^3 mol^{-1} K per cobalt ion at 330 K, essentially equal to the value expected for independent $S = \frac{3}{2}$ cobalt(II) centres with a sensible g value.[20] Cooling the sample causes a steadily more rapid decrease in $\chi_M T$, which reaches 0.2 cm^3 mol^{-1} K at 4 K (Fig. 4). The shape

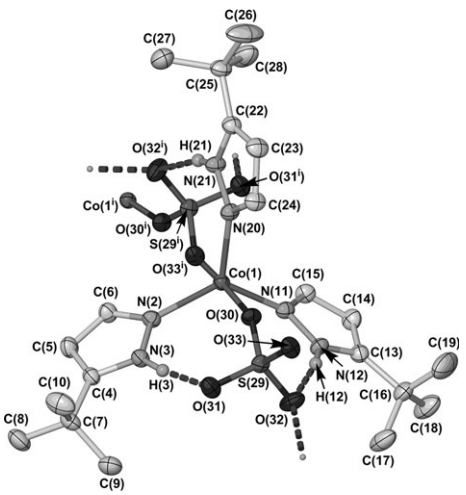

Fig. 1 View of the cobalt coordination sphere in the crystal structure of **1**. Thermal ellipsoids are at the 50% probability level and all carbon-bound hydrogen atoms have been deleted for clarity. Symmetry code: (i) $1-x, -\frac{1}{2}+y, \frac{3}{2}-z$.

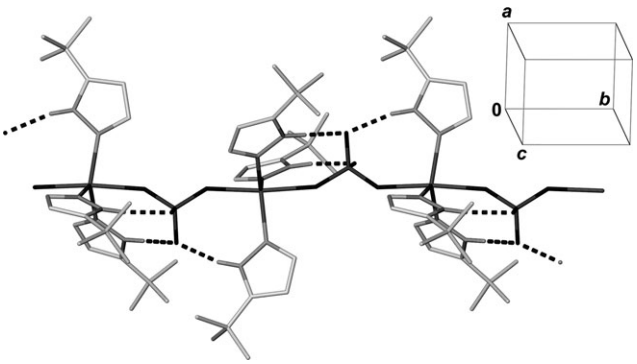

Fig. 2 View of the 1-D chain structure of **1**. All atoms have arbitrary radii. The unit cell orientation is shown in the inset (not to scale).

of this curve is typical of polynuclear cobalt(II) species, and is expected to contain contributions from antiferromagnetic exchange within the chain and zero-field splitting of the cobalt(II) spin manifold. The data obey the Curie–Weiss law throughout the temperature range studied, with $g = 2.37(1)$ and $\theta = -42.5(9)$ K.[20]

In principle, the orbital singlet $^4A'_2$ ground state expected from the trigonal bipyramidal cobalt centres in **1** (in idealised D_{3h} symmetry) means that they should be well-described by a magnetically-isotropic Heisenberg chain model. However, small distortions towards tetragonality in these compounds split the degenerate e' and e'' d-energy levels, which can introduce a significant degree of magnetic anisotropy into the system. This means that, in practice, small structural changes may have a profound effect on the symmetry of the g tensor and the sign of D in such compounds.[21,22]

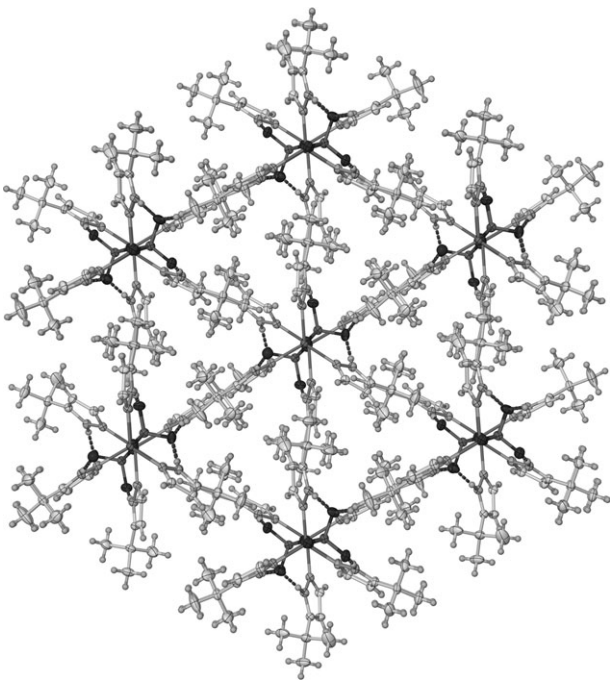

Fig. 3 Partial packing diagram of **1** perpendicular to the coordination polymer chains, showing their arrangement into a near-regular hexagonal array separated by interdigitated *tert*-butyl groups. The view is along the (010) crystal plane with the [101] vector vertical.

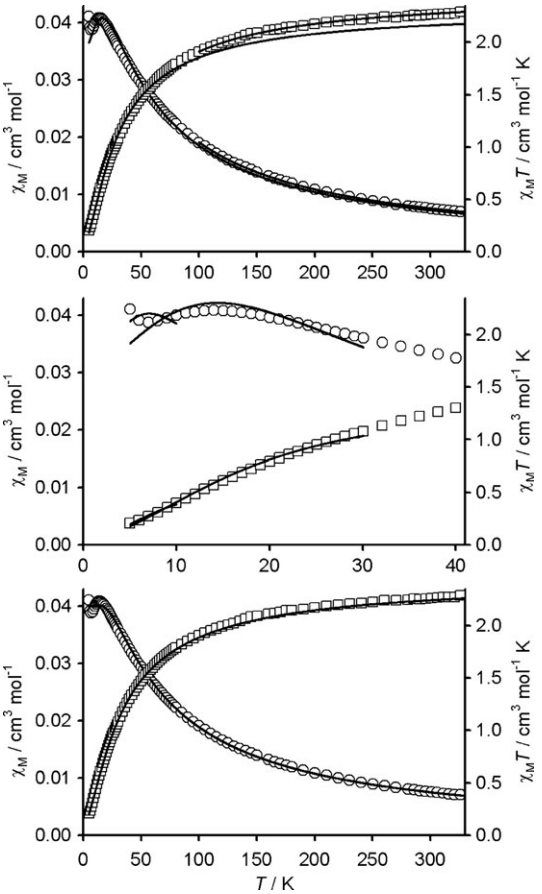

Fig. 4 Variable temperature magnetic susceptibility data for **1** per cobalt ion, plotted as χ_M (○) and $\chi_M T$ (□) *vs.* *T*. The lines show the best fits of the χ_M *vs.* *T* data to eqn. (1) for all data and $T > 100$ K (top), to eqn. (3) for $T < 30$ K and $T < 10$ K (centre), and to eqn. (5) (bottom). See Table 2 for fitting parameters.

Importantly, the low *g* value shown by **1** (*ca.* 2.4) and the fact that its magnetic data can be well-reproduced by Heisenberg treatments, as described below, both imply that magnetic anisotropy is small in this material.[22] If **1** did show significant magnetic anisotropy, then a substantially higher *g* factor of 3–4 would be expected.[1,23]

The magnetic data for **1** were first modelled by Fisher's expression for a Heisenberg chain of spins (eqn. (1) and eqn. (2), $S = \frac{3}{2}$).[6]

$$\chi_M = \frac{Ng^2\beta^2 S(S+1)}{3\,kT} \times \frac{1+u}{1-u} \qquad (1)$$

$$u = \coth\left[\frac{2JS(S+1)}{kT}\right] - \left[\frac{kT}{2JS(S+1)}\right] \qquad (2)$$

Modelling the χ_M *vs.* *T* data over the entire temperature range using this equation led to the parameters listed in Table 2. The resultant fit reproduced the χ_M *vs.* *T* plot well, but significantly underestimated $\chi_M T$ at higher temperatures (Fig. 4, top). This was reflected in a derived *g* value significantly below that predicted by the Curie–Weiss law (Table 2). Omitting the data from this analysis below 30, 50 or 100 K, which should be the most strongly affected by ZFS, resulted in only small changes

Table 2 Magnetic fitting parameters for **1**. *J* values are quoted according to a $H = -2J(S_1S_2)$ Hamiltonian

Method	*g*	J/cm^{-1}	$\lvert D\rvert$/cm^{-1}
Eqn. (1), all data	2.23(1)	−3.19(3)	—
Eqn. (1), $T > 100$ K	2.30(2)	−3.61(3)	—
Eqn. (3), $T < 30$ K	4.12(6)	−7.7(2)	—
Eqn. (3), $T < 10$ K	2.8(2)	−3.8(4)	—
Eqn. (5), all data	2.3(1)	−3.60(1)	22.9(3)

to *J*, but afforded a steadily increasing value of *g* and a consequent improvement in the high temperature fit to the $\chi_M T$ data (Table 2, Fig. 4). Increasing the low temperature cut-off above 100 K had no further influence on the fitted parameters, within experimental error.

Secondly, the low temperature magnetic data were modelled by Bonner and Fisher's equation describing an antiferromagnetic Heisenberg chain of $S = \frac{1}{2}$ spins (eqn. (3) and eqn. (4)).[24]

$$\chi_M = \frac{Ng^2\beta^2}{kT} \times \frac{0.25 + 0.074975x + 0.075235x^2}{1 + 0.9931x + 0.172135x^2 + 0.757825x^3} \qquad (3)$$

$$x = \frac{2|J|}{kT} \qquad (4)$$

The results of this calculation were strongly dependent on the high temperature cut-off used (Table 2, and Fig. 4, centre). Using data at $T < 30$ K afforded *J* and *g* values that were both significantly larger than those found from the earlier analysis, with *g* deviating strongly from that expected from the Curie constant of the material. The fitted parameters both decreased markedly as the cut-off temperature was lowered, towards the values obtained by eqn. (1). However, even when the analysis was restricted to $T < 10$ K, the value of *g* provided by eqn. (3) was significantly higher than expected from the Curie–Weiss law.

Finally, the complete magnetic data set was analysed using Rueff's approach (eqn. (5)):

$$\chi_M = \frac{A\exp\left(\frac{-E_1}{kT}\right) + B\exp\left(\frac{-E_2}{kT}\right)}{T} \qquad (5)$$

where $D = E_1$, $J = -E_2$ and $A + B = 5Ng^2\beta^2/4k$.[12] This equation reproduced the χ_M and $\chi_M T$ curves well over the whole temperature range (Fig. 4, bottom). Although this good agreement may reflect the fact that eqn. (5) is effectively a three parameter model, compared to the two-parameter models above, the correspondence between the *g* and *J* values yielded by this method and by the high temperature fit to eqn. (1) is striking (Table 2).

Conclusion

Despite its empirical nature, eqn. (5) appears to be the method of choice to model magnetic data from **1**, and probably from other cobalt(II) chain complexes as well. Results obtained from eqn. (1) and eqn. (5) are remarkably consistent, as long as only high temperature data (that are not significantly affected by ZFS) are included in the former analysis. Eqn. (5) avoids that ambiguity and also provides a determination of *D*. Results

from eqn. (3) did not agree with the other two approaches, presumably because the premise that only the $m_S = \pm\frac{1}{2}$ sub-levels are populated in **1** at low temperatures is not valid, even at 10 K.[3,25] This is consistent with eqn. (3) yielding results that approached the other methods more closely, as more high temperature data were omitted. Alternatively, however, since a susceptibility analysis cannot give the sign of D, it might be that D is positive rather than negative. In that case, the low-lying $m_S = \pm\frac{3}{2}$ sub-levels would be populated at low temperatures, making the assumptions behind the treatment in eqn. (3) invalid. Single crystal EPR studies of mononuclear, high-spin trigonal bipyramidal cobalt(II) complexes have afforded D values that are either positive or negative, depending on quite subtle structural factors.[21]

Experimental

3{5}-*Tert*-butylpyrazole (**L**) was synthesised by a literature procedure,[18] while all other reagents and solvents were purchased commercially and used as supplied.

A solution of $CoSO_4 \cdot 7H_2O$ (0.39 g, 1.38 mmol), **L** (0.51 g, 4.11 mmol) and NaOH (0.055 g, 1.38 mmol) was stirred in MeOH (30 cm^3) for 6 h. The deep purple solution was filtered and concentrated *in vacuo* to *ca.* 5 cm^3. Slow diffusion of Et_2O vapour into the solution gave purple crystals. Yield 0.33 g, 45%. Found: C, 47.5; H, 6.8; N, 16.0. Calc. for $C_{21}H_{36}CoN_6O_4S$: C, 47.8; H, 6.9; N, 15.9%.

Single crystal X-ray structure determination

Crystal data for **1**: $C_{21}H_{36}CoN_6O_4S$, M_r = 527.55, orthorhombic, $P2_12_12_1$, a = 10.7470(2), b = 13.1706(2), c = 18.1220(4) Å, V = 2565.07(8) Å^3, Z = 4, μ(Mo-K$_\alpha$) = 0.788 mm^{-1}, T = 150(2) K, 35 378 measured reflections, 5834 independent, R_{int} = 0.060, $R_1(F)$ = 0.031, w$R_2(F^2)$ = 0.077, Flack parameter 0.196(11).

Diffraction data were collected with a Nonius KappaCCD area detector diffractometer fitted with an Oxford Cryosystems low temperature device using graphite-monochromated Mo-K$_\alpha$ radiation (λ = 0.71073 Å). The structure was solved by direct methods (SHELXS96[26]) and developed by full least-squares refinement on F^2 (SHELXL96[27]). The crystal was refined as a racemic twin. No disorder was detected during refinement and no restraints were applied. All non-hydrogen atoms were refined anisotropically, while all hydrogen atoms were placed in calculated positions and refined using a riding model. Crystallographic figures were prepared using XSEED,[28] which incorporates POVRAY.[29]

While the ADSYMM routine in PLATON[30] suggested the alternative space group *Pnma* for **1**, transformation of the data into this higher symmetry space group and re-refinement of the structure led to a noisy model with highly unsatisfactory residuals [w$R_2(F^2)$ = 0.61]. Examination of the diffraction data showed that *hk*0 reflections with *h* odd, and 0*kl* reflections with $k + l$ odd, which would be systematically absent in *Pnma*, were often weak but were consistently observed. Therefore, this apparent higher symmetry is an artifact and our refinement in $P2_12_12_1$ is appropriate.

CCDC 646395. For crystallographic data in CIF or other electronic format see DOI: 10.1039/b700987a

Other measurements

C, H and N microanalyses were carried out by the University of Leeds School of Chemistry microanalytical service. Magnetic susceptibility measurements were obtained using a Quantum Design SQUID magnetometer in an applied field of 1000 G. Diamagnetic corrections were estimated from Pascal's constants.[20] All magnetochemical calculations and graph drawing were carried out using SIGMAPLOT.[31] No paramagnetic impurity or TIP terms were included in these analyses.

Acknowledgements

The authors thank Dr H. J. Blythe (University of Sheffield) for the susceptibility data, and the Leverhulme Trust for funding.

References

1 O. Kahn, *Molecular Magnetism*, VCH, Weinheim, Germany, 1993, pp. 251–263.
2 R. Boča, *Coord. Chem. Rev.*, 2004, **248**, 757.
3 A. V. Palii, B. S. Tsukerblat, E. Coronado, J. M. Clemente-Juan and J. J. Borrás-Almenar, *J. Chem. Phys.*, 2003, **118**, 5566.
4 M. E. Lines, *J. Chem. Phys.*, 1971, **55**, 2977.
5 M. Gerloch, *Prog. Inorg. Chem.*, 1979, **26**, 1.
6 M. E. Fisher, *Am. J. Phys.*, 1964, **32**, 343.
7 W. Hiller, J. Strähle, A. Datz, M. Hanack, W. E. Hatfield, L. W. Ter Haar and P. Gütlich, *J. Am. Chem. Soc.*, 1984, **106**, 329.
8 See, for example: (*a*) B.-Q. Ma, S. Gao, T. Yi and G.-X. Xu, *Polyhedron*, 2001, **20**, 1255; (*b*) T.-F. Liu, D. Fu, S. Gao, Y.-Z. Zhang, H.-L. Sun, G. Su and Y.-J. Liu, *J. Am. Chem. Soc.*, 2003, **125**, 13976; (*c*) M. B. Hursthouse, M. E. Light and D. J. Price, *Angew. Chem., Int. Ed.*, 2004, **43**, 472; (*d*) K.-L. Zhang, Y. Xu and X.-Z. You, *Transition Met. Chem.*, 2005, **30**, 376; (*e*) J.-M. Shi, Z. Liu, Y.-M. Sun, L. Yi and L.-D. Liu, *Chem. Phys.*, 2006, **325**, 237.
9 (*a*) D. B. Losee, J. N. McElearney, G. E. Shankle, R. L. Carlin, P. J. Cresswell and W. T. Robinson, *Phys. Rev. B*, 1973, **8**, 2185; (*b*) S. Foner, R. B. Frankel, W. M. Reiff, H. Wong and G. J. Long, *J. Chem. Phys.*, 1978, **68**, 4781.
10 J. N. McElearney and S. Merchant, *Phys. Rev. B: Solid State*, 1978, **18**, 3612.
11 See, for example: (*a*) M. K. Ehlert, A. Storr and R. C. Thompson, *Can. J. Chem.*, 1993, **71**, 1412; (*b*) G. De Munno, T. Poerio, M. Julve, F. Lloret and G. Viau, *New J. Chem.*, 1998, **22**, 299; (*c*) M. James and J. Horvat, *J. Phys. Chem. Solids*, 2002, **63**, 657; (*d*) J. M. Clemente-Juan, E. Coronado, A. Gaita-Ariño, C. Giménez-Saiz, H.-U. Güdel, A. Sieber, R. Bircher and H. Mutka, *Inorg. Chem.*, 2005, **44**, 3389.
12 (*a*) J.-M. Rueff, N. Masciocchi, P. Rabu, A. Sironi and A. Skoulios, *Eur. J. Inorg. Chem.*, 2001, 2843; (*b*) J.-M. Rueff, N. Masciocchi, P. Rabu, A. Sironi and A. Skoulios, *Chem.–Eur. J.*, 2002, **8**, 1813.
13 See, for example: (*a*) A. Majumder, V. Gramlich, G. M. Rosair, S. R. Batten, J. D. Masuda, M. S. El Fallah, J. Ribas, J.-P. Sutter, C. Desplanches and S. Mitra, *Cryst. Growth Des.*, 2006, **6**, 2355; (*b*) S. C. Manna, A. K. Ghosh, J. Ribas, M. G. B. Drew, C.-N. Lin, E. Zangrando and N. R. Chaudhuri, *Inorg. Chim. Acta*, 2006, **359**, 1395; (*c*) A. Beghidja, P. Rabu, G. Rogez and R. Welter, *Chem.–Eur. J.*, 2006, **12**, 7627.
14 X. Liu, J. A. McAllister, M. P. de Miranda, E. J. L. McInnes, C. A. Kilner and M. A. Halcrow, *Chem.–Eur. J.*, 2004, **10**, 1827 and references therein.
15 S. L. Renard, I. Sylvestre, S. A. Barrett, C. A. Kilner and M. A. Halcrow, *Inorg. Chem.*, 2006, **45**, 8711 and references therein.
16 L. F. Jones, K. D. Camm, C. A. Kilner and M. A. Halcrow, *CrystEngComm*, 2006, **8**, 719 and references therein.
17 L. F. Jones, C. A. Kilner, M. P. de Miranda, J. Wolowska and M. A. Halcrow, *Angew. Chem., Int. Ed.*, 2007, **46**, 4073.
18 S. Trofimenko, J. C. Calabrese and J. S. Thompson, *Inorg. Chem.*, 1987, **26**, 1507.

19 A. W. Addison, T. N. Rao, J. Reedijk, J. van Rijn and G. C. Verschoor, *J. Chem. Soc., Dalton Trans*., 1984, 1349.
20 C. J. O'Connor, *Prog. Inorg. Chem*., 1982, **29**, 203.
21 (*a*) C. Benelli and D. Gatteschi, *Inorg. Chem*., 1982, **21**, 1788; (*b*) C. Benelli, D. Gatteschi and G. Speroni, *Inorg. Chim. Acta*, 1984, **90**, 179.
22 M. J. Hossain and H. Sakiyama, *Inorg. Chim. Acta*, 2002, **338**, 255.
23 B. A. Goodman and J. B. Raynor, *Adv. Inorg. Chem*., 1970, **13**, 135.
24 J. C. Bonner and M. E. Fisher, *Phys. Rev*., 1964, **135**, A640.
25 O. Kahn, *Molecular Magnetism*, VCH, Weinheim, Germany, 1993, pp. 43.
26 G. M. Sheldrick, *Acta Crystallogr., Sect. A: Found. Crystallogr*., 1990, **46**, 467.
27 G. M. Sheldrick, *SHELXL-97, Program for refinement of crystal structures*, University of Göttingen, Germany, 1997.
28 L. J. Barbour, *J. Supramol. Chem*., 2003, **1**, 189.
29 *POVRAY v. 3.5*, Persistence of Vision Raytracer Pty. Ltd, Williamstown, Victoria, Australia, 2002, http://www.povray.org.
30 A. L. Spek, *J. Appl. Crystallogr*., 2003, **36**, 7.
31 *SIGMAPLOT, v. 8.02*, SPSS Scientific Inc.,Chicago IL, 2002.

